POAC'23
Glasgow, United Kingdom

Proceedings of the 27th International Conference on
Port and Ocean Engineering under Arctic Conditions
12-16 June 2023, Glasgow, UK

Detailed Spatial Temporal Analysis of Caspian Sea Ice Thickness Distribution Based on Differentiated FDD

Anton Sigitov[1], Yevgeniy Kadranov[1], Sergey Vernyayev[1], Irina Vernyayeva[1]
[1] ICEMAN.KZ LLP (Almaty, Kazakhstan)

ABSTRACT

Ice season severity index is usually described with accumulated Freezing Degree Days (FDD) in a particular area. Daily average air temperatures comprising FDD were derived by ICEMAN.KZ for various zones of the Caspian Sea from ERA-5 reanalysis data with modifications to account for ground measurements in the region. Spatial variation of the index enabled control of the thermal ice thickness growth model using growth rates associated with varying air temperature regime. Ice cover displacement tracking floes from the place of origin to other zones recorded daily increased accuracy of ice thickness estimation. These records were compiled into a hindcast database for winter seasons starting from 2005 that is used to assess hazards for operations in ice, describe interaction mechanisms with offshore structures and to quantify impact. Seasonal variation of ice thickness and how ice masses are distributed over the sea are discussed in the paper.

KEY WORDS: Caspian Sea; FDD; Ice thickness; Regional ice monitoring.

NOMENCLATURE

ERA5 (latest climate reanalysis produced by ECMWF), FDD (Freezing Degree Days), IPCC (Intergovernmental Panel on Climate Change), KHM (KazHydroMet), RHM (RosHydroMet).

INTRODUCTION

Caspian Sea is in the mid-latitudes between Europe and Asia. Despite the significant distance to the Arctic, the geographical peculiarity of the region is absence of any elevated obstacles that could serve as a barrier for Arctic cold air masses on the way to the area through Siberia. Seasonally forming ice cover is thus regulated with temporary regular cold snaps varying in duration and intensity through a season's length and from year to year. Figure 1 illustrates such spatial variation during a random cold snap in 2016. The coldest area was Northeast of the sea and its intensity gradually reduced through the Northern part of the sea to Southwest. The most affected parameter characterizing ice cover properties and thus development of ice conditions through the season and spatially across the sea is ice thickness. Thus, classification of winter severity by FDD was first introduced by Terziev et al. (1992) to differentiate ice cover development for various types of winters. This is the first historical data source that has introduced seasonal variability of ice thickness for several observation posts along the northern coast of the Caspian.

With the collapse of Soviet Union, Russian research institutions focused on Volga Delta, whereas Kazakhstan sector of the sea was mainly monitored and studied by commercial companies focusing on corporate needs of Oil & Gas exploration in the early 2000s. Most modern studies have restricted access and are not generally available to the public. Most importantly researchers have concentrated on distinctive peculiarities of ice thickness growth and trends within their limited study areas.

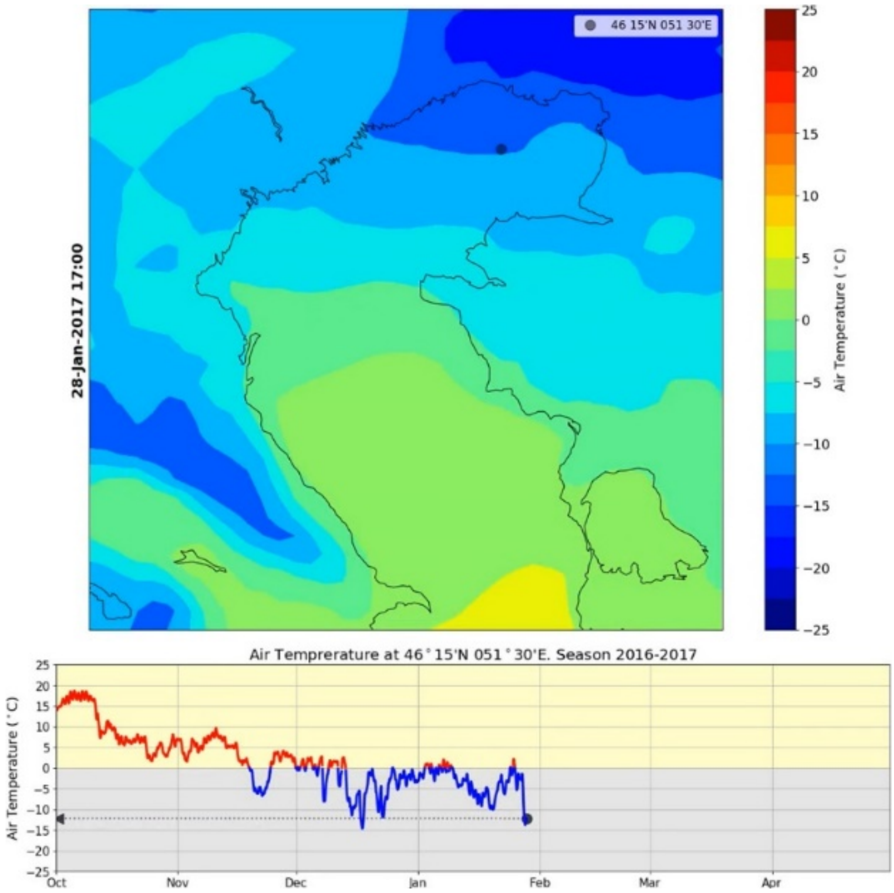

Figure 1 Example of air temperature variation across the Caspian region during a cold snap associated with cold air masses intrusion in the region. Full timelapse of the variation is available at Iceman Youtube Channel (2023).

Vernyayev et al. (2023a) have considered the whole Northern part of the Caspian Sea when compiling ice cover classification database. Their approach to management of air temperature records in grid over the whole region enabled aggregating Freezing Degree Days (FDD) for discrete forecast zones. Daily observations supported with remote sensing data allowed defining freeze-up dates and detailed ice cover classification through each season tracking origin of ice cover formation and inherited accumulated freezing degree days as ice masses drift from one forecast zone to the other. Thus, spatial variability of ice thickness distribution over the whole Caspian Sea was recorded for the observation period from 2005 to 2023 with further plans to extend dataset to 2000.

This paper is dedicated to ice thickness component of the database briefly describing the background calculations and empirical thermal model. The resulting dataset is used to present variability of ice thickness across the region. This type of analysis with the level of detail and precision has never been performed in the region.

ICE THICKNESS GROWTH MODEL

The model was developed to support daily ice cover classification hindcast activities. The goal was to numerically estimate realistic ice growth rate per day for each zone where ice has formed from day one and onwards until the end of the season. The air temperature grid compiled as described by Vernyayev et al. (2023a) was the main input data source for thermal calculations. Calculation of ice thickness was performed using daily average air temperature derived from the grid for each forecast zone as introduced in the hindcast program. Remote sensing data and interpretation of ice cover composition by partial concentrations were the main triggers to initiate calculation of up to three ice thicknesses per forecast zone.

Shokr and Sinha (2015) heat-balance equation (1) for ice thickness growth Δh_i on a N-th day from freeze-up date was used as a basis for calculation approach.

$$(\Delta h_i)_N = \frac{k_i k_s}{L_i \rho_i}\left[\frac{T_w-(T_a)_N}{k_s(h_i)_{N-1}+k_i(h_s)_N}\right], \text{ [cm]} \quad (1)$$

Where k_i and k_s is the thermal conductivity of ice and snow, L_i is the latent heat of ice, ρ_i is ice density, T_w – freeze-up temperature of water, $(T_a)_N$ is the average daily air temperature on N-th day, $(h_i)_{N-1}$ is a previous day ice thickness, $(h_s)_N$ is a thickness of snow cover on N-th day.

This model of ice thickness growth was selected as the closest solution to consider both negative air temperature for growth during cold snaps and positive or near zero temperature during thaw periods that are typical for the region. Several experiments have also confirmed that additional components for solar radiation and geothermal energy effects are critical for the period from February 15 until the end of winter. The first one constitutes melting due to geography of the Caspian being in the midlatitudes. The second one is considered due to shallow waters in the north-eastern part and becomes significant during the break-up period when temperature gradient is negligible.

Exploratory phase has also identified analytical solution did not give consistent result from season to season due to quality of the source data. The general shape of the equation was used to derive an empirical formula instead with A and B coefficients controlling speed of growth and erosion. Equation (2) is the final look of the empirical formula coded into the hindcast program.

$$(\Delta h_i)_N = A\left[\frac{T_w-(T_a)_N}{k_s(h_i)_{N-1}+k_i(h_s)_N}\right] - B, \text{ [cm/day]} \quad (2)$$

T_w=-0.9°C for brackish water. This value varies together with salinity from season to season depending on water volumes gained from Volga. This variation is within 0.4°C and requires more effort to define than added value from increased accuracy that is not likely to be achieved due to even higher spatial variability across the Northern part of the Sea.

Coefficients A and B were calibrated based on comparison with measurements at ground stations published by RosHydroMet (RHM) and KazHydroMet (KHM) in the landfast zones along the Northern coastline and at Kulaly Island in the archipelago of Seal Islands closer to typical Ice Edge. A is roughly $5.6*10^{-3}$ J*cm/(°C^2*s*days) considering k_s=0.25 J/m°Cs, k_i=2 J/m°Cs at the first iteration of experiments during calibration and adjusted for 70% of measurements. This coefficient describes reasonable ice thickness growth during moderate negative temperatures. Larger values are used for rapid growth during cold snap periods and lower during near zero temperatures.

Coefficient B varies from 0.1-0.2 cm/day in the middle of February and reaches 1-3 cm/day by the end of March to account for increasing intensity of sun radiation. Snow thickness h_s is assigned 5 cm thickness for the first cold week after snow coverage was defined from MODIS data. It is assumed that water saturation of snow masses, especially in the second half of a season, reduces its insulating properties. There is also a theory that was confirmed with observation of ice cross-section in the field that snow cover constitutes to ice thickness growth with melt water generation during day under effect of sun that freezes during colder nights. This theory is yet to be confirmed with more detailed monitoring and measurements in the field.

Wave induced erosion near ice edge or when low concentrations of ice cover are combined with high wind events are managed with manual modification of Coefficient B to account for rapid ice thickness deterioration.

Ice thickness model verification

Ice thickness model verification was performed at the initial stages of Caspian hindcast program design. There are three data sources that contributed most to the activity. Preferably drilled thickness measurements were used in the verification if acquisition method was known. The first one is RosHydroMet's meteorological database (ESIMO, 2022) that contains records from ports in Volga Delta and most importantly ports offshore side of Delta. The second source is KazHydroMet (KazHydroMet, 2023) and their records of landfast ice thickness at Peshnoi Island (just offshore from the Ural River mouth at the Northern coast) and limited measurements from Kulaly (banana shaped island near typical ice edge). The third source is internal measurements performed by the group at any opportunity. These are detailed and consider a variety of ice cover ages and origins. But they are not numerous.

Physical measurements were plotted as time series per season per location together with daily average air temperature observed near the measurement sites model output and their corresponding A and B coefficients. A basic one component ice thickness estimation model based on FDD accounting only for negative air temperature was plotted alongside for comparison of results. Figure 2 illustrates resulting model performance and variation of A and B components after curve fitting exercise.

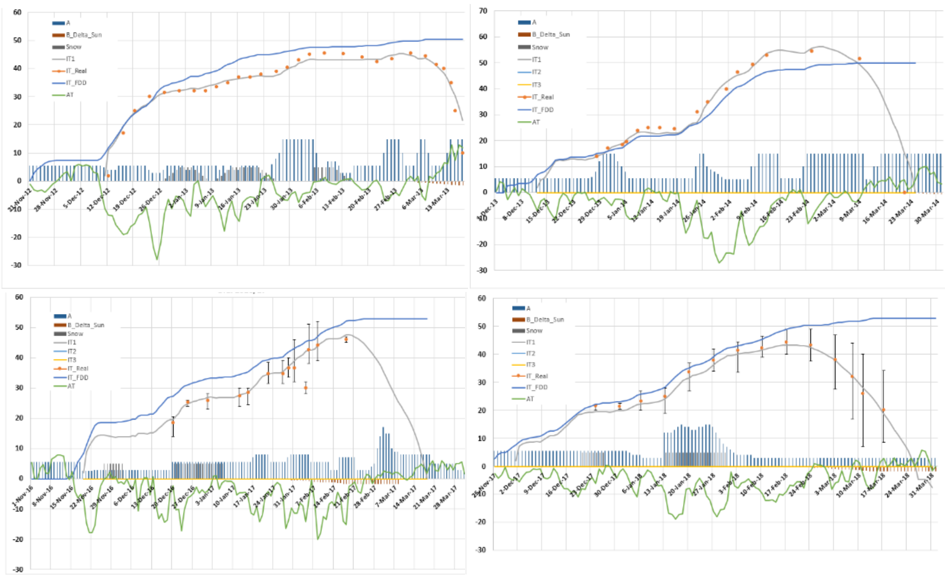

Figure 2 Examples of thermal model performance verification with physical measurements data and comparison with model considering only negative degree days.

A and *B* coefficients were recorded with more than 150 exercises for various sites and seasons encompassing all types of winters by severity. Resulting records were compared with daily average gradient to build a regression function controlling choice of empirical coefficients based on air temperature value and intensity of cold snap intrusion indicated by the gradient.

The model's performance and accuracy were deemed tolerable for the purpose of the hindcast program. Most importantly the model was assessed through ice charting operations based on many seasons compiled into the hindcast database. On most instances, unsupervised ice thickness calculation based on season's record of air temperature reached the melting point coinciding with confirmed disappearance of ice cover in a forecast zone. It has served as a reliable performance indicator for the group.

Data Acquisition and Interpretation

When performing ice cover classification analysis operators use pre-calculated ice thicknesses for each area of homogeneous ice conditions to assign up to three thickness values in each polygon. Automatic quality assurance routine prevents submission of day's observation until all polygons are updated and verified versus current conditions. When physical observations are available in a forecast zone, they are displayed on a graph of estimated ice thickness enabling operators to manually override pre-configured A and B coefficients to account for weather conditions that the model has not seen before. New values are fed to the regression model to teach it for new circumstances. This routine ensures acquired data is consistent and knowledge is captured to re-use for the following analysis and forecasts.

Caspian Sea hindcast data is regularly refined into a 1×1 km grid to analyze spatial distribution of ice cover parameters. This iteration creates temporally and spatially consistent timeseries in every grid cell over the region that enables aggregation of statistical descriptors for various periods and building scenario-based window of opportunity or persistence analysis.

Following the monitoring program and standards used to gather ice thickness data, each grid cell includes at least one and maximum three daily ice thickness values representing various stages of ice development with associated partial ice concentrations within the area of the cell. Maximum thickness is normally the oldest ice either formed within or drifted into the area. Figure 3 shows resulting records of ice thickness distributed by their coverage over a zone in the northeastern part of the sea.

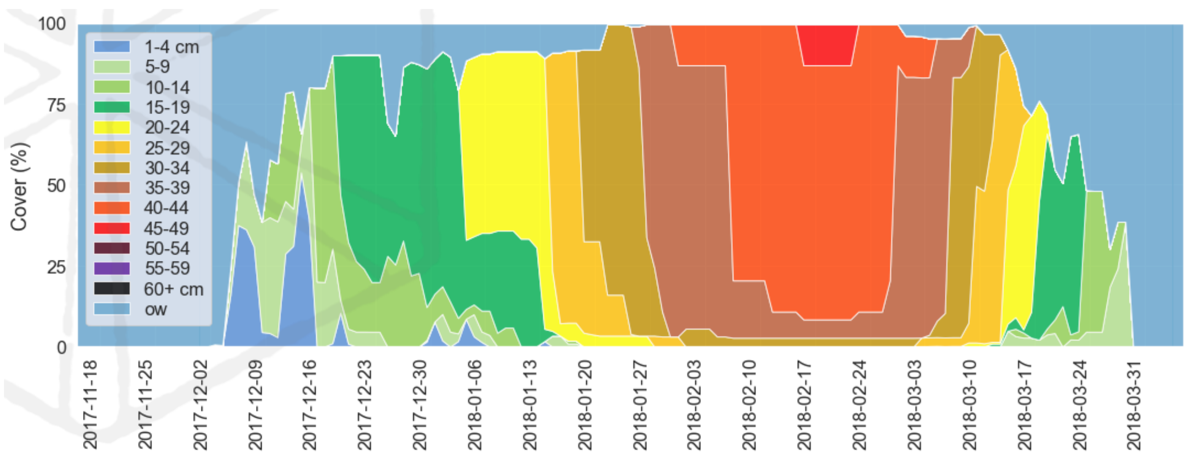

Figure 3 Timeseries of ice thickness distribution by concentration in a forecast zone of the Northeastern Caspian.

Monitoring three ice thicknesses introduces increased flexibility of ice thickness observations to deliver more detailed insights for specifics of applications where it is used as an event descriptor. Thus, for example, two types of maximum ice thickness values are considered in the scope of standard statistical output generated as pre-built ice environment statistical report for the region:

- Absolute maximum is the thickest ice observed in an area regardless of its concentration. Distributions with this value are representative of the worst-case scenario and are conservative. Even 1/10th partial concentration in an area of delineated homogeneous ice conditions will be picked by aggregation algorithm disregarding possibility that the second and third thicknesses may be significantly lower. This value is comparable with ice thickness derived from FDD in majority of pre-coastal areas with dominating landfast ice.
- Weighted average maximum is the value achieved during a season in an area and weighted by areal concentration observed in an area. Distributions with this value are more realistic as they are representative of ice thickness corresponding to the predominant stage of development in an area.

Although ice thickness analysis becomes more complicated with introduction of additional indicators this flexibility enables choosing statistical description suitable for specifics of analysis. Thus, the second aggregate is used in this paper to present ice thickness variation across the Caspian Sea for the period of available observations. A daily analogue of this aggregate is used to estimate ice volume. Ice volume trends being closely correlated to air temperature trends enable direct connection of climate change indexes to effects on operations from ice thickness. When all ice cover parameters in the database are considered based on a scenario of interaction for a specific structure or an operation a quantified climate change impact assessment can be performed based on long-term predictions. IPCC (2014) outlooks can be used as input for this analysis, for example.

CASPIAN SEA ICE THICKNESS

Available observations from 2005 to 2022 can be divided into two periods before (colder) and after (warmer) 2013. Different rates of seasonal Ice Volume as summarized by Vernyayev et al. (2023b) and most importantly Water Level reduction, generally warmer seasons during the second period, different types of ice events (mobility of ice cover as described in Sigitov et al. (2023)), seasonal ice cover development and different distribution of ice features characterize the two periods.

Spatial distribution of ice thickness in the region

Figure 4 summarizes spatial distribution of aggregated weighted average ice thickness for the period from 2005 to 2022. Distributions in the bottom are compiled following conventional engineering requirements to analyze as much data as available for a region. The top figures illustrate the same values with observations from 2013 to 2022 with previous period's colder winters omitted. The latter is representative of conditions answering pessimistic global warming predictions with continued growth of regional air temperature.

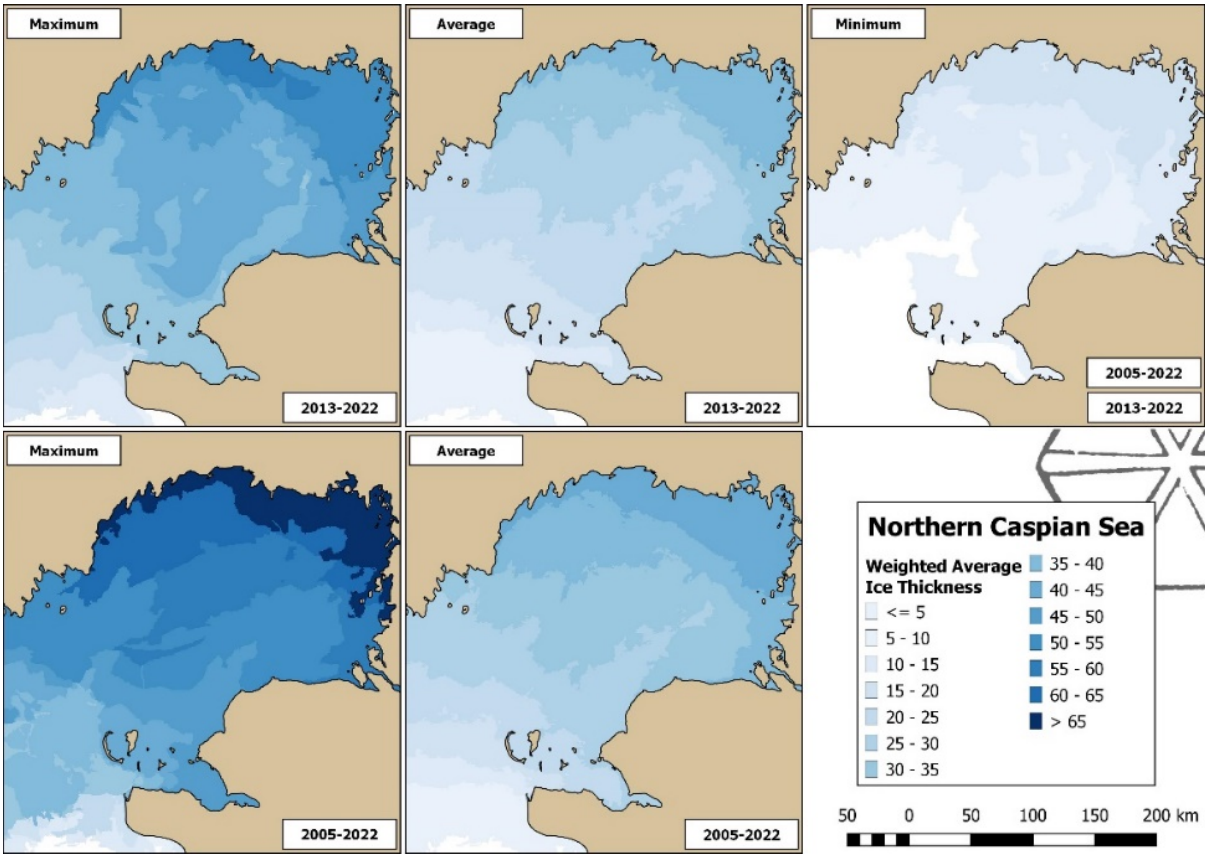

Figure 4 Spatial distribution of maximum average and minimum of seasonal thickest weighted average ice thicknesses observed in periods from 2013 to 2022 (top) and from 2005 to 2022 (bottom).

The maximum weighted average ice thickness values in each cell per season as observed during considered periods were used to derive corresponding maximum average and minimum values. Note the maximum values along the Northeastern coastline may coincide with absolute maximums that are derived disregarding partial concentrations. This is the area where landfast ice zone is typical and there is less drift that may result in opening leads or temporary break-up. Thus, there is less chance that second or third thicknesses appear through a season.

High variability between minimum and maximum values illustrates the result of inter-seasonal variability and persistence of cold air intrusion events into the region. Gradient reduction of average ice thickness from North-East to Southwest corresponds to typical patterns of cold air intrusion events. First, frequency of such events reduces in the Western part of the Sea. Secondly, intensity of events is leveled with water reservoir balancing significant gradient of temperatures. It should be noted that the Eastern part of the sea is fully covered with immobile ice as reported by Sigitov et al. (2023) during severe winters. When the sea surface is covered with thick solid ice cover it has the least effect on air masses moving across the region. Severe negative air temperature reaches the mid Caspian and the Western coast in this case. This leads to rapid ice cover growth in front of Volga delta, ice edge extending into the mid Caspian and drifting ice along both Eastern and Western coasts reaching Aktau and Baku. The history of observations in the region indicates that the last severe winter following Terziev et al. (1992) classification occurred in 2011-2012 as illustrated with freezing degree days record in Figure 5.

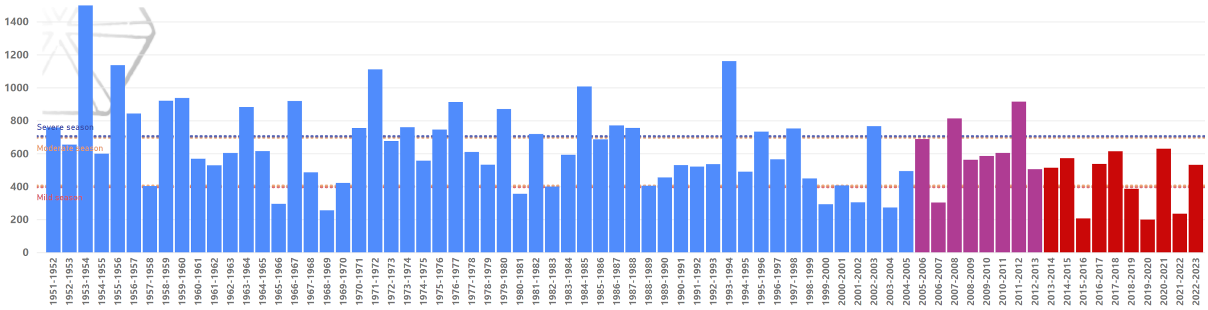

Figure 5 Freezing Degree Days accumulated over a forecast zone in the Northeastern part of the Caspian Sea as observed from 1951 to 2023.

The difference of ice thickness spatial distribution for the two reference periods points out the importance of records duration and correct choice of reference period for purpose of studies. This is the most important for an ice load estimation. For example, ice thickness input to load calculation based on 2013-2022 period may be considered conservative for design of structures planned for deployment in 20-30 years from now with current IPCC (2014) projections. However, 2005-2022 includes the extreme season that should be considered for manned structures designed to perform hazardous operations following ISO guidelines. Finding the right balance to ensure safety of operations at the right cost is now possible with data driven decision.

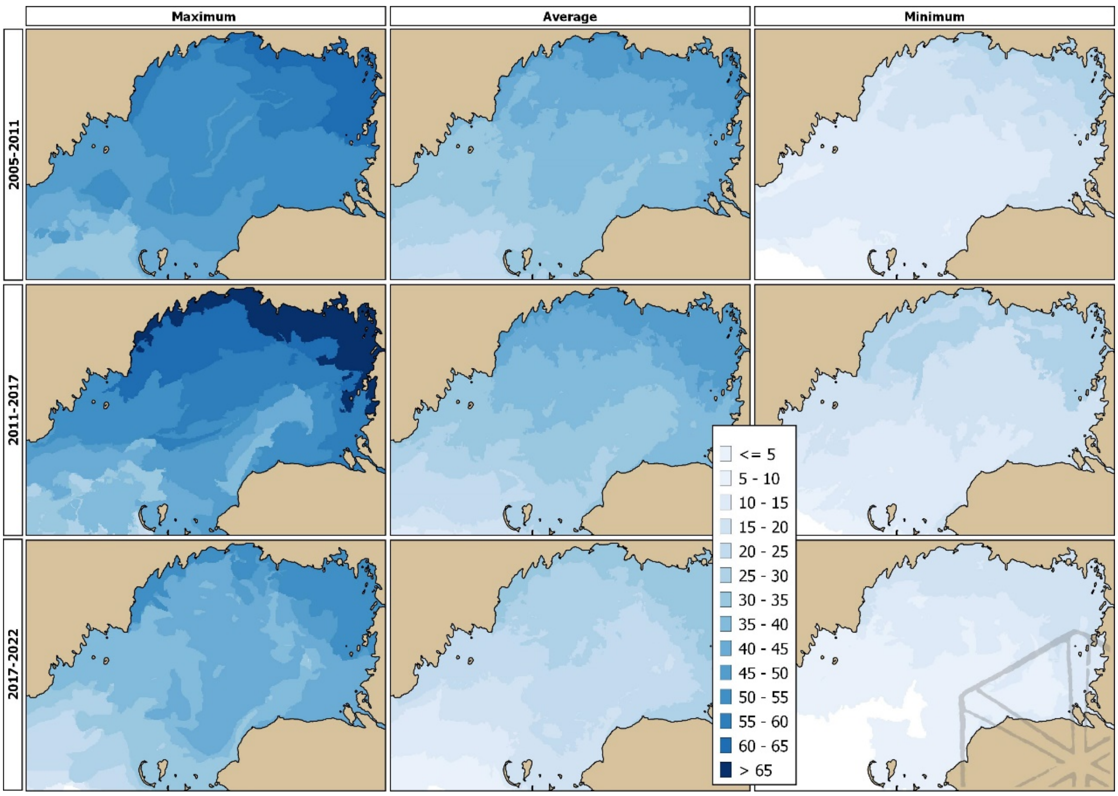

Figure 6 Spatial distribution of maximum average and minimum of seasonal thickest weighted average ice thicknesses observed in three discrete periods from 2005 to 2022.

Further exploration of discrete periods within the dataset indicates that spatial coverage of thicker ice on average was continuously declining through the length of the period as illustrated with charts in the middle of Figure 6 above. The last five years this reduction was the most dramatic with pre-coastal thickest ice along the northern shore dropping by 10 cm. Severe season in 2011-2012 as obvious with the most intensive color might have affected the averaged values for 2011-2017 period resulting in smaller difference between the first two.

Monthly distribution of ice thickness

Monthly distributions of the thickest ice (left) and weighted average ice thickness (right) for two forecast zones in the Northeastern part of the sea are summarized for the two considered periods in Figure 7. Absolute maximum thicknesses are aggregated regardless of their partial concentration. Quartiles (Turney, 2023) indicate the number of occurrences through month in each cell of 1×1km grid. Weighted average ice thicknesses quartiles can be referred to forecast zone area coverage per month.

The spread of values from the average has increased during the later warmer period, suggesting increased mobility of ice cover, periodic clearance of sea surface and consequent growth of ice in both zones. Although maximum thicknesses achieved each month and observed at offshore forecast zone (blue) are similar to those in pre-coastal zone (beige), distributions show higher averages and frequency of thicker ice occurrence corresponding to pre-coastal ice.

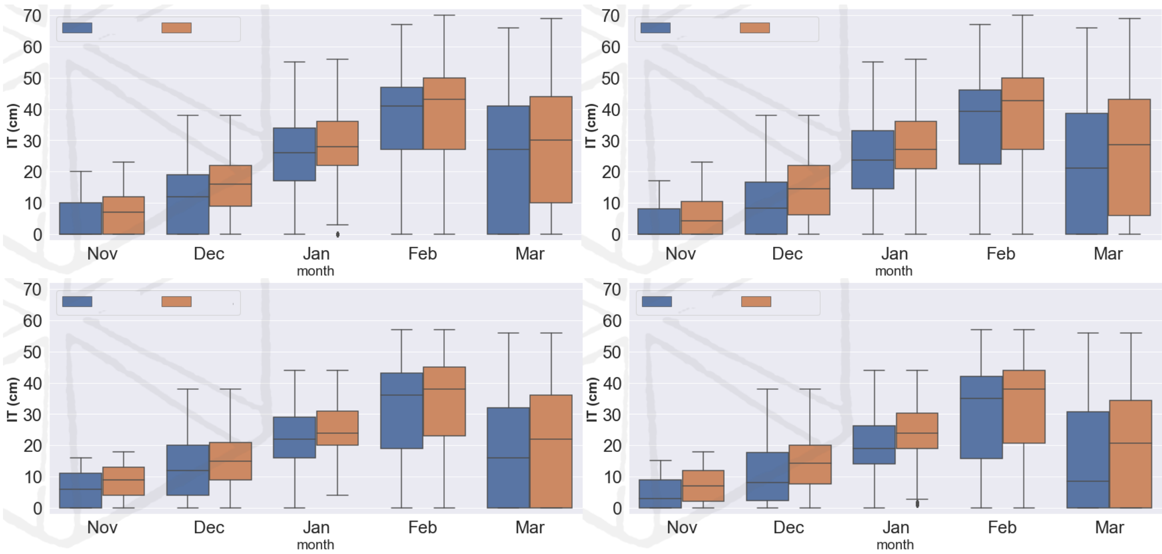

Figure 7 Monthly distributions of the thickest (left) ice thickness and weighed average ice thickness (right) values for periods from 2005 to 2022 (top) and from 2013 to 2022 (bottom) at two forecast zones (blue – offshore with mobile ice conditions orange – pre-coastal with dominating stable ice cover) in the northeastern part of the sea. See Dutoit (2012) for box plot visualization of quartiles.

OTHER APPLICATIONS

As ice thickness is one of the key parameters for ice regime description, it is used for multiple operational, engineering and research applications.

Break-up forecast enhancement

Breakup forecast for the Caspian Sea is a regular service provided by ICEMAN.KZ. One of the key features used in breakup forecast is ice volume trends. Ice volume is estimated as a product of ice thickness and ice cover. While remote sensing data can provide relatively straightforward estimates of ice coverage, more accurate ice thickness estimates as described above enable precise track of ice volume through season development. Precise ice volume records enable more accurate choice of analogous seasons and modelling based on recognized patterns of ice cover response to weather development.

Ice – structures interaction and impact assessments

Ice thickness data described in this paper was also used as input for structures design and their deployment feasibility assessment over large area. Demonstrated spatial variability of ice thickness across the region facilitated the study with more informative impact assessment and insights on structures' response to interaction with ice cover through variable ice loads, pile-up heights and ride-up intrusion distance estimates. Ice thickness data with corresponding concentration, floe sizes and metocean parameters was used to develop interaction scenarios. The history of observations in line with other ice and metocean parameters enabled probabilistic assessment of impact using the scenarios.

Simulation of marine transport performance in ice infested waters

Ice thickness data was also used as one of the input parameters for simulating marine transport performance in the Caspian Sea. Shallow waters of the Caspian Sea make in-ice navigation sensitive to ice thickness variability. This application of ice thickness data is covered in Kadranov et al. (2023).

Offshore operational planning and forecasting

Spatial distribution of ice thickness plays significant role to plan offshore operations with low ice class vessels and barges outside of normal routines. Combination of mobility, ice thickness and projections based on weather forecast are basis for ice hazard assessments and search of window of opportunity. Accounting for cross-drift in channels through shallow waters, formation of ridges along the track, closure or opening of leads makes such evaluations an overwhelming and informative insight on safety of planned missions. Thus, a data driven decision can be made for a Go or Stand Down. Similar types of assessments are performed for evacuation availability monitoring with lighter crafts that are subject to limiting ice conditions.

CONCLUSIONS

This paper contains detailed description of ice thickness variability in the North Caspian Sea and recently observed trend associated with changing environment. Spatial distribution of ice thickness values across Caspian Sea was demonstrated for the period starting from 2005 to 2022. A clear reduction trend of ice thickness in general and spatially by intensity was observed. The effect of extremely mild winters and generally warmer moderate winters during the last ten years demonstrated the cause. Existing projections on climate change indicate further reduction of ice thickness can be expected in the region. The effects are further elaborated by Vernyayev et al (2023b) where analysis of ice volume change as a derivative of ice thickness illustrates the trends and shows effects on operations and marine mammals' habitat.

Data acquisition process, ice growth model description and verification process were addressed illustrating synergy of remote sensing data interpretation, empirical modeling and analytical solutions for thermal growth of ice.

ACKNOWLEDGEMENTS

This activity was only possible due to Copernicus project (https://www.copernicus.eu/en) as a part of EU space program which provides valuable publicly available data for our work such as images from Sentinel constellations and ERA5 climate weather data. The second but no less important contributor is NASA space program providing free access to MODIS and Landsat remote sensing data. Without such programs our work would not be possible, and their open data approach is highly valued in our group.

REFERENCES

Dutoit S. H. C. 2012. Graphical Exploratory Data Analysis. Springer.

ESIMO 2022 [online]. Data. Available at: http://esimo.ru/portal/ [Accessed June 2022].

ICEMAN.KZ [online]. Available at: https://www.ice-service.net/ru/caspian-sea [Accessed 01 March 2023].

Iceman Youtube Channel [online]. Air Temperature Development across the Caspian Sea. Winter Season 2016-2017. Available at: https://youtu.be/Pw8oFZSyZlw. [Accessed 01 March 2023].

IPCC, Barros, V.R., C.B. Field, D.J. Dokken, M.D. Mastrandrea, K.J. Mach, T.E. Bilir, M. Chatterjee, K.L. Ebi, Y.O. Estrada, R.C. Genova, B. Girma, E.S. Kissel, A.N. Levy, S. MacCracken, P.R. Mastrandrea, and L.L.White (eds.). 2014. 'Climate Change 2014: Impacts, Adaptation, and Vulnerability. Part B: Regional Aspects. Contribution of Working Group II to the Fifth Assessment Report of the Intergovernmental Panel on Climate Change'. Cambridge, United Kingdom and New York, NY, USA.

Kadranov Y., Vernyayev S., Sigitov A., 2023, Marine Units Performance Simulation under changing environment in the Caspian Sea. *Proceedings of the 27th International Conference on Port and Ocean Engineering under Arctic Conditions*, June 12-16, Glasgow, UK, POAC23.

KazHydroMet [online] Annual Caspian Hydrological Regime data from KazHydroMet, available at: https://www.kazhydromet.kz/ru/kaspiyskoe-more/ezhegodnye-dannye-o-rezhime-kaspiyskogo-morya [Accessed 10 January 2023]

Sigitov A., Kadranov Y., Vernyayev S., Vernyayeva I., 2023, Caspian Ice Cover Mobility. *Proceedings of the 27th International Conference on Port and Ocean Engineering under Arctic Conditions*, June 12-16, Glasgow, UK, POAC23.

Shokr M., Sinha N.K., 2015. *Sea Ice. Physics and Remote Sensing.* John Wiley & Sons, Inc., Hoboken, New Jersey.

Terziev P. S., Kosarev A.N., Kerimova A.A., 1992 *Hydrometeorology and hydrochemistry of seas. Caspian Sea*. Hydrometeoizdat: Saint-Petersburg.

Turney, S. 2023, Quartiles & Quantiles | Calculation, Definition & Interpretation. Scribbr. Retrieved March 29, 2023, from https://www.scribbr.com/statistics/quartiles-quantiles/.

Vernyayev S., Kadranov Y., Sigitov A., Vernyayeva I., 2023a, Caspian Sea Ice Cover Hindcast Database. *Proceedings of the 27th International Conference on Port and Ocean Engineering under Arctic Conditions*, June 12-16, Glasgow, UK, POAC23.

Vernyayev S., Sigitov A., Kadranov Y., Vernyayeva I., 2023b, Caspian Seasonal Ice Volume Trends in Recent History. *Proceedings of the 27th International Conference on Port and Ocean Engineering under Arctic Conditions*, June 12-16, Glasgow, UK, POAC23.